

# Rectified Gaussian Scale Mixtures and the Sparse Non-Negative Least Squares Problem

Alican Nalci, Igor Fedorov, and Bhaskar D. Rao

**Abstract**—In this paper we introduce a hierarchical Bayesian framework to obtain sparse and non-negative solutions to the sparse non-negative least squares problem (S-NNLS). We introduce a new family of scale mixtures, the Rectified Gaussian Scale Mixture (R-GSM), to model the sparsity enforcing prior distribution for the signal of interest. One advantage of the R-GSM prior is that through proper choice of the mixing density it encompasses a wide variety of heavy tailed distributions, such as the rectified Laplacian and rectified Student’s t distributions. Similar to the Gaussian Scale Mixture (GSM) approach, a Type II Expectation-Maximization framework is developed to estimate the hyper-parameters and obtain a point estimate of the parameter of interest. In the proposed method, called rectified Sparse Bayesian Learning (R-SBL), both the E-step and M-step are carried out in closed form. Finally through numerical experiments we show that R-SBL outperforms existing S-NNLS solvers in terms of both signal and support recovery.

**Index Terms**—Non-negative Least Squares, Bayesian Sparse Signal Recovery, Rectified Gaussian Scale Mixtures

## I. INTRODUCTION

In this paper we consider a linear system of equations of the form

$$\mathbf{y} = \Phi \mathbf{x} + \mathbf{v} \quad (1)$$

where the solution of interest,  $\mathbf{x} \in \mathbb{R}_+^M$ , is assumed to be non-negative. The matrix  $\Phi \in \mathbb{R}^{N \times M}$  is fixed and related to the underlying physical problem,  $\mathbf{y} \in \mathbb{R}^N$  is the measurement vector, and  $\mathbf{v}$  is the additive measurement noise modeled as a zero mean Gaussian random vector with uncorrelated entries, i.e.  $\mathbf{v} \sim \mathcal{N}(0, \sigma^2 \mathbf{I})$ . Recovering the optimal solution to (1) is known as solving the non-negative least squares (NNLS) problem. NNLS has received considerable attention in the context of methods for solving systems of linear equations [1], density estimation [2], compressive non-negative imaging [3], and non-negative matrix factorization (NMF) [4], [5], [6], among others. Non-negative data is also a natural occurrence in many application areas, such as text mining [7], image processing [8], speech enhancement [9], and spectral decomposition [10], [11] and requires special consideration. To this end, we pose the solution to the NNLS problem in (1) as

$$\underset{\mathbf{x} \geq 0}{\text{minimize}} \quad \|\mathbf{y} - \Phi \mathbf{x}\|_2. \quad (2)$$

The authors are with the Department of Electrical and Computer Engineering, University of California, San Diego, La Jolla, CA 92092 USA (nalci@eng.ucsd.edu; ifedorov@eng.ucsd.edu; brao@ucsd.edu)

This work was partially supported by KIET of MOTIE grant funded by Korea government in 2015. [No. 10050527, General-purpose module, sensor and system development projects to enhance industrial safety network]

Igor Fedorov work was partially supported by the ARCS Foundation.

In many applications,  $N < M$  and, therefore, (1) is under-determined. As a result, a unique solution to (2) may not exist. However, recovering an exact solution is possible if additional information is known about the solution. A useful assumption, and one that has been recently made in many applications, is that the solution is sparse [12], [13], [14]. The problem becomes more well-posed if  $\mathbf{x}$  is known to be sparse, i.e. has few non-zero elements. In this case, (2) is simply modified to

$$\underset{\mathbf{x} \geq 0, \mathbf{y} = \Phi \mathbf{x}}{\text{minimize}} \quad \|\mathbf{x}\|_0 \quad (3)$$

where  $\|\mathbf{x}\|_0$ , the  $\ell_0$  pseudo-norm, is the number of non-zero elements in  $\mathbf{x}$ . We will refer to (3) as the sparse NNLS (S-NNLS) problem.

Directly solving (3) is not tractable, since the  $\ell_0$  pseudo-norm is not convex in its arguments and the problem is NP-hard in general [15]. Therefore greedy algorithms have been suggested to approximate the solution [15], [16]. One example is the class of algorithms known as Orthogonal Matching Pursuit (OMP) [17], which successively select non-zero elements of  $\mathbf{x}$  in a greedy fashion. In order to adapt OMP to the S-NNLS problem, the criterion by which a new non-zero element of  $\mathbf{x}$  is selected is modified to select the one having the largest *positive* value [18]. Another approach in this class of algorithms first finds an  $\mathbf{x}$  such that  $\|\mathbf{y} - \Phi \mathbf{x}\|_2 \leq \epsilon$  and  $\mathbf{x} \geq 0$  using the active-set Lawson-Hanson algorithm [1] and then prunes  $\mathbf{x}$  with a greedy procedure until  $\|\mathbf{x}\|_0 \leq K$ , where  $K$  is a pre-specified desired sparsity [4].

Greedy algorithms are computationally attractive to solve NP-hard problems, but often lead to sub-optimal solutions [15]. Thus, numerous convex relaxations of the  $\ell_0$  penalty have been considered as an alternative to greedy methods [15]. One simple alternative is to replace the  $\ell_0$  penalty with  $\ell_1$  and cast the problem in (3) as

$$\underset{\mathbf{x} \geq 0}{\text{minimize}} \quad \|\mathbf{y} - \Phi \mathbf{x}\|_2 + \lambda \|\mathbf{x}\|_1 \quad (4)$$

where  $\lambda > 0$  is a suitably chosen regularization parameter. The advantage of this formulation is that it is in the form of a constrained convex optimization problem and can be solved by any number of methods [19], [20]. One approach is to estimate  $\mathbf{x}$  through a projected gradient descent procedure [21]. Whereas the projected gradient descent procedure requires a line-search in order to calculate the learning rate at each iteration, the approach can be simplified by employing a multiplicative update rule which guarantees a decrease in (4) at each iteration [22]. In fact, the  $\ell_1$  norm penalty in (4) can

be replaced by any sparsity inducing regularization function  $g(\mathbf{x})$ :

$$\underset{\mathbf{x} \geq 0}{\text{minimize}} \quad \|\mathbf{y} - \Phi \mathbf{x}\|_2 + \lambda g(\mathbf{x}). \quad (5)$$

For instance, [23], [24] consider  $g(\mathbf{x}) = \sum_{i=1}^M \log(x_i^2 + \beta)$ , which leads to an iterative re-weighted optimization approach.

An alternative and more promising view on the S-NNLS problem is to cast the entire problem in a Bayesian framework and consider the maximum a-posteriori (MAP) estimate of  $\mathbf{x}$  given the data  $\mathbf{y}$ :

$$\mathbf{x}_{MAP} = \arg \max_{\mathbf{x}} p(\mathbf{x}|\mathbf{y}). \quad (6)$$

There is a strong connection between the Bayesian framework in (6) and deterministic formulations like the one in (5): it has recently been shown that formulations of the form in (5) are equivalent to the formulation in (6) with the proper choice of prior  $p(\mathbf{x})$  [25]. For example, considering a separable  $p(\mathbf{x})$  of the form

$$p(\mathbf{x}) = \prod_{i=1}^M p(x_i), \quad (7)$$

the  $\ell_1$  regularization approach in (4) is equivalent to the Bayesian approach in (6) with an exponential prior for  $p(x_i)$ . In this paper, our emphasis will be on Bayesian approaches to solving (1).

#### A. Contributions of the Paper

- We introduce a novel class of sparsity inducing priors for the S-NNLS problem, namely priors modeled as a rectified Gaussian Scale Mixture (R-GSM). These are an extension of the Gaussian Scale Mixture (GSM) model [26], [27], [28], [29] and represent a large class of heavy tailed priors appropriate for inducing sparsity.
- We cast the S-NNLS problem in a Bayesian framework using R-GSM priors and develop a Type II inference procedure, which we call Rectified Sparse Bayesian Learning (R-SBL). We develop a detailed Bayesian inference procedure for estimating  $\mathbf{x}$  using the Expectation-Maximization (EM) algorithm. We detail two potential point estimate strategies for R-SBL: the mean and mode point estimates. Moreover, we provide closed form expressions for the probabilistic quantities of interest.
- We demonstrate the utility of the R-GSM prior and efficacy of the R-SBL algorithm with extensive experimental results comparing the proposed technique to existing S-NNLS algorithms. We also discuss the robustness of the proposed method in the case of noisy measurements.

#### B. Organization of the Paper

In the following sections, we provide details of the proposed R-SBL algorithm. In Section II, we discuss the advantages of scale mixture priors for  $p(\mathbf{x})$  and introduce the R-GSM prior. In Section III, we define the Type I and Type II Bayesian approaches to solve the S-NNLS problem and introduce the main R-SBL framework with R-GSM prior. We provide details of an EM technique for estimating  $\mathbf{x}$  in Section III-B, with

derivations presented in Appendix VI-A, VI-B, and VI-C. We present experimental results comparing the proposed R-SBL algorithm to existing methods in Section IV. Finally, we conclude the work in Section V.

## II. RECTIFIED GAUSSIAN SCALE MIXTURES

In this work, we assume separable priors of the form (7) and focus on the choice of  $p(x_i)$ . The choice of prior is very important because it plays a central role in the Bayesian inference procedure. For the problem at hand, the prior must be sparsity inducing, satisfy the non-negativity constraint, be general and versatile enough to be widely applicable, and tractable for simplicity of algorithm development. Consequently, we consider the scale mixture prior:

$$p(x_i) = \int_0^\infty p(x_i|\gamma_i)p(\gamma_i)d\gamma_i. \quad (8)$$

Scale mixture priors were first considered in the context of GSM's [26]. It is well known that super-gaussian densities are the best priors for promoting sparsity [30], [31] and most such priors can be represented in the form shown in (8), with the proper choice of  $p(\gamma_i)$  [32], [33], [29], [28], [27]. This has made GSM based priors a valuable form of prior for the general sparse signal recovery problem. Another advantage of the scale mixture prior is that it establishes a Markovian structure of the form

$$\gamma \rightarrow \mathbf{x} \rightarrow \mathbf{y}$$

where inference can be performed in the  $\mathbf{x}$  domain (MAP or Type I) and also in the  $\gamma$  domain (Type II). This provides additional flexibility and opportunity to explore algorithm development. Experimental results in the standard sparse signal recovery problem show that performing inference in the  $\gamma$  domain consistently achieves superior performance [25], [30]. The performance gains may be due to the intuition that  $\gamma$  is deeper in the Markovian chain than  $\mathbf{x}$ , so the influence of errors in performing inference in the  $\gamma$  domain may be diminished [25], [34], [35]. At the same time,  $\gamma$  is close enough to  $\mathbf{y}$  in the Markovian chain such that meaningful inference about  $\gamma$  can still be performed [25].

Although priors of the form shown in (8) have been used widely in the compressed sensing literature (where the signal model is identical to (1) without the non-negativity constraint) [25], this framework has not been extended to the S-NNLS problem. In [36], a Rectified Gaussian (RG) prior is considered for  $p(x_i)$  within a variational bayesian inference framework. Our goal in this work is to develop a more flexible and general class of priors. Considering the findings that the scale mixture prior is superior to most existing sparse signal recovery algorithms [25], we propose a R-GSM prior for the S-NNLS problem, where  $p(x_i|\gamma_i)$  in (8) is given by the RG distribution. We refer to the proposed inference framework with R-GSM prior as Rectified Sparse Bayesian Learning (R-SBL).

The RG distribution is defined as

$$\mathcal{N}^R(x|\mu, \gamma) = \sqrt{\frac{2}{\pi\gamma}} \frac{1}{\operatorname{erfc}\left(-\frac{\mu\sqrt{\gamma}}{\sqrt{2}}\right)} e^{-\frac{(x-\mu)^2}{2\gamma}} u(x)$$

where  $\mu$  is the location parameter,  $\gamma$  is the scale parameter,  $u(x)$  is the unit step function, and  $\text{erfc}(x)$  is the complementary error function, defined as

$$\text{erfc}(x) = \frac{2}{\sqrt{\pi}} \int_x^\infty e^{-t^2} dt.$$

When  $\mu = 0$ , the RG density becomes

$$\mathcal{N}^R(x|0, \gamma) = 2\mathcal{N}(x|0, \gamma)u(x) = \sqrt{\frac{2}{\pi\gamma}} e^{-\frac{x^2}{2\gamma}} u(x). \quad (9)$$

As noted in [37], [38], closed form inference computations using scale mixtures of RG's is tractable only if the location parameter is zero, which effectively makes the  $\text{erfc}(\cdot)$  vanish. Thus, in this work, we focus on R-GSM with  $\mu = 0$ .

Motivated by Gaussian Scale mixtures, we use the RG prior in a scale mixture framework in order to provide a general and flexible class of priors and to better promote *sparse* non-negative solutions. R-GSM priors have the form

$$p(x) = \int_0^\infty \mathcal{N}^R(x|0, \gamma) p(\gamma) d\gamma. \quad (10)$$

Different choices of  $p(\gamma)$  lead to different choices of priors. A few examples are presented below.

#### A. Examples of R-GSM Representation of Sparse Prior

A random variable modeled by a R-GSM can also be viewed as generating a random variable with a GSM and then taking its absolute value. This allows one to leverage the GSM prior literature to develop the class of R-GSM priors.

For instance, consider the following exponential, or rectified Laplacian, prior for  $x$

$$p_e(x) = \lambda e^{-\lambda x} u(x).$$

By using an exponential prior for  $p(\gamma)$ ,

$$p(\gamma) = \frac{\lambda^2}{2} e^{-\frac{\lambda^2 \gamma}{2}} u(\gamma) \quad (11)$$

we can express  $p_e(x_i)$  in the R-GSM form [39] as

$$\begin{aligned} p_e(x) &= 2u(x) \int_0^\infty \mathcal{N}(x|0, \gamma_i) \frac{\lambda^2}{2} e^{-\frac{\lambda^2 \gamma}{2}} u(\gamma) d\gamma \\ &= \lambda e^{-\lambda x} u(x). \end{aligned}$$

Likewise, by considering the R-GSM with  $p(\gamma)$  given by the Gamma( $a, b$ ) distribution, we get a rectified student-t distribution for  $p(x)$ . In this case, (8) simplifies to [30]

$$\begin{aligned} p(x) &= 2u(x) \int_0^\infty \mathcal{N}(x|0, \gamma) \frac{\gamma^{a-1} e^{-\frac{\gamma}{b}}}{a^b \Gamma(a)} d\gamma \\ &= \frac{2b^a \Gamma(a + \frac{1}{2})}{(2\pi)^{\frac{1}{2}} \Gamma(a)} \left( b + \frac{x^2}{2} \right)^{-(a + \frac{1}{2})} u(x) \end{aligned}$$

where  $\Gamma$  is defined as

$$\Gamma(a) = \int_0^\infty t^{a-1} e^{-t} dt.$$

More generally, all of the distributions represented by the GSM have a corresponding rectified version represented by a R-GSM, e.g. contaminated Normal and slash, symmetric stable and logistic, hyperbolic, etc. [29], [28], [27], [26], [32] [33].

### III. BAYESIAN INFERENCE WITH SCALE MIXTURE PRIOR

There are two Bayesian approaches for solving the S-NNLS problem with a scale mixture prior. The first approach, called Type I estimation (MAP) performs inference in the  $\mathbf{x}$  domain by treating  $\gamma$  as the hidden variable. On the other hand, the second approach, called Type II, performs inference in the  $\gamma$  domain. We briefly discuss Type I in the next section and the major portion of the paper is dedicated to Type II estimation because of its observed superiority in standard sparse signal recovery problems [25].

#### A. Type I or MAP estimation

Employing Type I to solve S-NNLS translates into calculating the maximum a-posteriori (MAP) estimate of  $\mathbf{x}$  given  $\mathbf{y}$ :

$$\arg \min_{\mathbf{x}} \|\mathbf{y} - \Phi \mathbf{x}\|_2^2 - \lambda \sum_{i=1}^M \log p(x_i). \quad (12)$$

Many of the  $\ell_0$  relaxation methods described in Section I can be re-derived from the Type I perspective. For instance, by choosing an exponential prior for  $p(\gamma_i)$ , leading to an exponential prior on  $p(x)$ , (12) reduces to the  $\ell_1$  regularization approach in (4) with the added benefit that  $\lambda$  has a probabilistic interpretation. Similarly, by choosing a Gamma prior for  $p(\gamma_i)$ , which corresponds to a rectified student-t prior on  $p(x_i)$ , (12) reduces to

$$\arg \min_{\mathbf{x}} \|\mathbf{y} - \Phi \mathbf{x}\|_2^2 + \lambda \sum_{i=1}^M \log \left( b + \frac{x_i^2}{2} \right)$$

which leads to the re-weighted  $\ell_2$  approach to the S-NNLS problem described in [23][24].

#### B. Type II Estimation: R-SBL for S-NNLS

The R-SBL framework aims to infer the hyper-parameters  $\gamma$  that shape the R-GSM prior. A MAP estimate of  $\gamma$  is computed and then the posterior density of interest  $p(\mathbf{x}|\mathbf{y})$  is approximated as  $p(\mathbf{x}|\mathbf{y}, \gamma_{MAP})$ . Having estimated the posterior density, appropriate point estimates can be readily obtained.

Based on past experience in Type II estimation for the standard sparse signal recovery problem, several strategies exist for estimating  $\gamma$ , two of which are presented here. In Section III-B1, we consider the problem of forming a MAP estimate of  $\gamma$  given  $\mathbf{y}$  by directly minimizing the appropriate posterior density. Section III-B2 shows how  $\gamma$  can be estimated by utilizing an EM framework. Finally, in Section III-B3, we discuss how to get a point estimate of  $\mathbf{x}$  given an estimate for  $\gamma$ .

1) *Inference of  $\gamma$  Using MAP Estimation:* The MAP estimate of  $\gamma$  is defined as

$$\gamma_{MAP} = \arg \max_{\gamma} p(\gamma | \mathbf{y}) = \arg \max_{\gamma} p(\mathbf{y} | \gamma) p(\gamma). \quad (13)$$

To carry out the estimation, one requires knowing  $p(\mathbf{y} | \gamma)$  or its suitable approximation. For the R-GSM prior, it turns out that  $p(\mathbf{y} | \gamma)$  has a closed form expression, which is derived

in Appendix VI-C. However, because of its complicated form and non-convex nature, optimization of  $p(\mathbf{y}|\gamma)$  or the log-likelihood does not appear to be straight-forward. Although Majorization-Minimization type approaches can be utilized, as was done for the GSM case, the process is still involved and is not pursued here any further. Tractable optimization methods in this vein will be a future research topic. Instead, we pursue an EM based procedure in Section III-B2, which turns out to be quite tractable.

2) *Inference using Expectation Maximization (EM)*: A more tractable approach is to estimate  $\gamma$  using EM, where we treat  $(\mathbf{x}, \mathbf{y}, \gamma)$  as the complete data, and treat  $\mathbf{x}$  as the hidden variable. The E-step involves determining  $Q(\gamma, \gamma^t)$ , which is defined as the conditional expectation of the complete log likelihood, as indicated below

$$Q(\gamma, \gamma^t) = E_{\mathbf{x}|\mathbf{y}, \gamma^t, \sigma^2} [\log p(\mathbf{y}|\mathbf{x}) + \log p(\mathbf{x}|\gamma) + \log p(\gamma)] \quad (14)$$

$$\doteq \sum_{i=1}^M E_{\mathbf{x}|\mathbf{y}, \gamma^t, \sigma^2} \left[ -\frac{1}{2} \log \gamma_i - \frac{x_i^2}{2\gamma_i} \right] \quad (15)$$

where  $t$  refers to the iteration index and  $\doteq$  refers to the fact that constant terms and terms which don't depend on  $\gamma$  have been omitted since they don't effect the maximization step. For the sake of simplicity of this paper, we also assume a non-informative prior on  $\gamma$ ,  $p(\gamma_i) = 1, \forall i$  [30]. This has been most effective in the GSM context and other priors, particularly log-concave priors, can be readily incorporated. Next, the M-step is carried out. For this, we maximize  $Q(\gamma, \gamma^t)$  with respect to  $\gamma$  by taking the derivative and setting it equal to zero, which yields an estimate of  $\gamma$  to be used in the next iteration:

$$\gamma_i^{t+1} = E_{\mathbf{x}|\mathbf{y}, \gamma^t, \sigma^2} [x_i^2]. \quad (16)$$

To calculate the expectation in (16), we need to derive the posterior  $p(\mathbf{x}|\mathbf{y}, \gamma, \sigma^2)$ . The posterior is given by

$$p(\mathbf{x}|\mathbf{y}, \gamma) = \frac{e^{-\frac{(\mathbf{x} - \boldsymbol{\mu})^T \boldsymbol{\Sigma}^{-1} (\mathbf{x} - \boldsymbol{\mu})}{2}}}{|\boldsymbol{\Sigma}|^{1/2} \left(\frac{\pi}{2}\right)^{M/2} \prod_{i=1}^M \operatorname{erfc}\left(-\frac{\beta_i}{\sqrt{2}}\right)} u(\mathbf{x}) \quad (17)$$

where  $\boldsymbol{\mu}$  and  $\boldsymbol{\Sigma}$  are readily given by [40], [30], [41] as

$$\boldsymbol{\mu} = \boldsymbol{\Gamma} \boldsymbol{\Phi}^T (\sigma^2 \mathbf{I} + \boldsymbol{\Phi} \boldsymbol{\Gamma} \boldsymbol{\Phi}^T)^{-1} \mathbf{y} \quad (18)$$

$$\boldsymbol{\Sigma} = \boldsymbol{\Gamma} - \boldsymbol{\Gamma} \boldsymbol{\Phi}^T (\sigma^2 \mathbf{I} + \boldsymbol{\Phi} \boldsymbol{\Gamma} \boldsymbol{\Phi}^T)^{-1} \boldsymbol{\Phi} \boldsymbol{\Gamma} \quad (19)$$

where  $\boldsymbol{\Gamma} = \operatorname{diag}(\gamma)$ . The full derivation of the posterior is provided in Appendix VI-A. Let  $\boldsymbol{\Sigma}^t = \mathbf{L}^t (\mathbf{L}^t)^T$  be the Cholesky decomposition of  $\boldsymbol{\Sigma}^t$  and  $\beta_i^t$  the entries of the vector  $\boldsymbol{\beta}^t = (\mathbf{L}^t)^{-1} \boldsymbol{\mu}^t$ . Then,  $E_{\mathbf{x}|\mathbf{y}, \gamma^t, \sigma^2} [x_i^2]$  can be expressed as

$$E_{\mathbf{x}|\mathbf{y}, \gamma^t, \sigma^2} [x_i^2] = \operatorname{diag}(\mathbf{L}^t \mathbf{R}^t (\mathbf{L}^t)^T)_i \quad (20)$$

where  $\operatorname{diag}(\cdot)_i$  is the  $i$ 'th entry of the main diagonal, and  $\mathbf{R}^t$  has elements  $R_{ij}^t$  given by

$$R_{ii}^t = (\beta_i^t)^2 + 1 + \sqrt{\frac{1}{\pi}} \frac{\beta_i^t e^{-\frac{(\beta_i^t)^2}{2}}}{\operatorname{erfc}\left(-\frac{\beta_i^t}{\sqrt{2}}\right)} \quad (21)$$

and

$$R_{ij}^t = \left( \beta_i^t + \sqrt{\frac{2}{\pi}} \frac{e^{-\frac{(\beta_i^t)^2}{2}}}{\operatorname{erfc}\left(-\frac{\beta_i^t}{\sqrt{2}}\right)} \right) \left( \beta_j^t + \sqrt{\frac{2}{\pi}} \frac{e^{-\frac{(\beta_j^t)^2}{2}}}{\operatorname{erfc}\left(-\frac{\beta_j^t}{\sqrt{2}}\right)} \right) \quad (22)$$

for  $i \neq j$ . The full derivation of  $E_{\mathbf{x}|\mathbf{y}, \gamma^t, \sigma^2} [x_i^2]$  is provided in Appendix VI-B.

The above equations are sufficient to implement the EM algorithm; Equation (20) is the E-step and equation (16) is the M-step.

3) *Point estimate of  $\mathbf{x}$* : Given  $\hat{\gamma}$ , the goal is to find a point estimate of  $\mathbf{x}$  from  $p(\mathbf{x}|\mathbf{y}, \hat{\gamma})$ . The optimal estimator of  $\mathbf{x}$  in the mean-square-error (MSE) sense is simply given by [42]

$$\hat{\mathbf{x}}_{mean} = E_{p(\mathbf{x}|\mathbf{y}, \hat{\gamma})} [\mathbf{x}] = \mathbf{L} \tilde{\boldsymbol{\mu}} \quad (23)$$

where  $\tilde{\boldsymbol{\mu}}_i$  is given by

$$\tilde{\boldsymbol{\mu}}_i = \beta_i + \sqrt{\frac{2}{\pi}} \frac{e^{-\frac{\beta_i^2}{2}}}{\operatorname{erfc}\left(-\frac{\beta_i}{\sqrt{2}}\right)}. \quad (24)$$

The full derivation of  $E_{p(\mathbf{x}|\mathbf{y}, \hat{\gamma})} [\mathbf{x}]$  is provided in Appendix VI-B.

An alternative point estimate is to use  $\hat{\mathbf{x}}_{mode}$ , given by

$$\begin{aligned} \hat{\mathbf{x}}_{mode} &= \arg \max_{\mathbf{x}} p(\mathbf{x}|\mathbf{y}, \hat{\gamma}) \\ &= \arg \min_{\mathbf{x} \geq 0} \|\mathbf{y} - \boldsymbol{\Phi} \mathbf{x}\|_2^2 + \lambda \sum_{i=1}^M \frac{x_i^2}{\gamma_i} \end{aligned} \quad (25)$$

where (25) can be solved by any NNLS solver.  $\hat{\mathbf{x}}_{mode}$  is a favorable point estimate because it chooses the peak of  $p(\mathbf{x}|\mathbf{y}, \hat{\gamma})$ , which could be multi-modal and not characterized well by its mean. Note that if all entries of  $\tilde{\boldsymbol{\mu}}$  are positive, then calculating (25) is not necessary as this point is the true mode, i.e.  $\hat{\mathbf{x}}_{mode} = \tilde{\boldsymbol{\mu}}$ . To see this recall that  $\tilde{\boldsymbol{\mu}}$  is the location parameter of a multivariate rectified Gaussian density with its peak residing on the positive orthant. However, this does not hold if any one of the entries of  $\tilde{\boldsymbol{\mu}}$  are negative.

The performance of both point estimate methods is discussed in Section IV.

### C. Complete Algorithm Description

The complete R-SBL method is summarized in Algorithm 1 for easy reference. Operators Cholesky and diag denote the Cholesky decomposition and constructing a matrix with diagonal entries as the argument vector, respectively. The algorithm works iteratively as it tries to maximize the conditional expectation in Equation (16).

## IV. EXPERIMENTS

In this section we provide two sets of experiments to show the recovery performance of the R-SBL approach. In the first set, we simulate a near 'noiseless' case where the noise has distribution  $\mathbf{v} \sim \mathcal{N}(\mathbf{0}, \sigma^2 \mathbf{I})$  with  $\sigma^2 = 10^{-6}$ . We do

**Require:**  $\mathbf{y}, \Phi, \sigma^2, \epsilon$

- 1: Initialize  $\Gamma^0 = \mathbf{I}$ ,  $t = 1$
- 2: **while**  $\frac{\|\gamma^{t-1} - \gamma^t\|_2}{\|\gamma^{t-1}\|_2} \geq \epsilon$  **do**
- 3:     Calculate  $\mu^t$  using (18) and  $\Gamma^{t-1}$
- 4:     Compute  $\Sigma^t$  using (19) and  $\Gamma^{t-1}$
- 5:     Compute  $\mathbf{L}^t = \text{Cholesky}(\Sigma^t)$
- 6:     Compute  $\beta^t = (\mathbf{L}^t)^{-1} \mu^t$
- 7:     Compute  $\mathbf{R}^t$  using  $\beta^t$ , (16), (21), and (22)
- 8:     Compute  $\gamma^{t+1} = \text{diag}(\mathbf{L}^t \mathbf{R}^t (\mathbf{L}^t)^T)$
- 9:      $t \leftarrow t + 1$
- 10: **end while**
- 11: Compute  $\tilde{\mu} = E_{\mathbf{x}|\mathbf{y}, \gamma, \sigma^2}[(\mathbf{L})^{-1} \mathbf{x}]$  and  $\mathbf{x} = \mathbf{L} \tilde{\mu}$  for mean estimator using (23) and (37), or compute  $\mathbf{x} = \hat{\mathbf{x}}_{mode}$  using (25) for mode estimator
- 12: **return**  $\mathbf{x}$

Fig. 1: R-SBL Algorithm

simulations for a wide variety of distributions for  $\mathbf{x}$  and  $\Phi$ . In the second set, we set the noise variance such that the signal to noise ratio (SNR) is 20 dB to test the robustness of the R-SBL approach under noisy conditions. In all of the cases, we compare our approach to available baseline S-NNLS solvers: SLEP- $\ell_1$  [43], and NN-OMP [44]. The noiseless case provides a fair comparison between the recovery performance of the S-NNLS solvers since, in this scenario, algorithm parameters are easy to select. In the noisy setting, tuning of various algorithm parameters leads to differing behavior of the algorithms, making it difficult to draw wide-reaching conclusions about the relative performance of the algorithms. Therefore, noisy simulations are meant for robustness analysis of R-SBL rather than comparison with other methods. Note that we use terms  $\mathcal{N}^R$  and RG interchangeably to denote the rectified Gaussian distribution.

#### A. Experiment Design

We generate sparse ground truth solutions  $\mathbf{x}^{gen} \in \mathbb{R}_+^{100}$  such that  $\|\mathbf{x}^{gen}\|_0 = K$ . We draw elements of  $\mathbf{x}^{gen}$  according to the following distributions:

- I. RG (Location: 0, Scale: 1)
- II. NN-Cauchy (Location: 0, Scale: 1)
- III. NN-Laplace (Location: 0, Scale: 1)
- IV. NN-Gamma (Location: 1, Scale: 2)
- V. Chi-square with  $\nu = 2$
- VI. Bernoulli with  $p(0.5) = 1/2$  and  $p(1.5) = 1/2$

where the prefix 'NN' stands for non-negative. The non-negative distributions are obtained by taking the absolute value of the respective probability densities, i.e. NN- $\mathbf{X} = |\mathbf{X}|$ .

Next, we randomly generate  $\Phi \in \mathbb{R}^{100 \times 400}$  according to the following densities

- I. Gaussian (Location: 0, Scale: 1)
- II.  $\pm 1$  with  $p(1) = 1/2$  and  $p(-1) = 1/2$

and we normalize the columns of  $\Phi$  to have unit  $\ell_2$  norm. For a given  $\Phi$  and  $\mathbf{x}^{gen}$ , we compute the synthetic measurements  $\mathbf{y} = \Phi \mathbf{x}^{gen}$  and use various S-NNLS algorithms to approximate  $\mathbf{x}^{gen}$  by  $\hat{\mathbf{x}}$ .

#### B. Performance Metrics

To evaluate the performance of S-NNLS algorithms, we use the mean squared recovery error (MSE) and the probability of error in the recovered support (PE), which are two commonly used performance metrics in the compressive sensing literature [15]. We measure the MSE between the recovered signal  $\hat{\mathbf{x}}$  and the ground truth  $\mathbf{x}^{gen}$  using

$$\text{MSE} = \frac{1}{N} \sum_{i=1}^N (\hat{x}_i - x_i^{gen})^2 \quad (26)$$

Denoting the support of the true solution as  $S$  and the support of  $\hat{\mathbf{x}}$  as  $\hat{S}$ , PE is calculated using

$$\text{PE} = \frac{\max\{|S|, |\hat{S}|\} - |S \cap \hat{S}|}{\max\{|S|, |\hat{S}|\}}. \quad (27)$$

A value of PE = 0 indicates that the ground truth and recovered supports are the same, whereas PE = 1 indicates no overlap between supports. Averaging the PE over multiple trials gives us the empirical probability of making errors in the support. We perform 1000 trials for each combination of distribution for  $\mathbf{x}^{gen}$ , distribution for  $\Phi$ , and cardinality  $K = \{1, 5, 10, 15, 20, 25, 30, 35, 40, 45, 50\}$ . Lastly, we calculate the average values of MSE and PE over 1000 trials. In the following sections, we use MSE and PE to indicate the averaged values.

#### C. Experiment Results

In this section we detail the experimental results, showing the benefits of R-SBL compared to other methods. The results will show that, in all of the sparse recovery experiments described, the proposed R-SBL method performs significantly better than its SLEP- $\ell_1$  and NN-OMP counterparts both in terms of MSE and PE.

Figures 2 and 3 show the MSE and PE as a function of solution cardinality, with elements of  $\Phi$  drawn from a normal distribution,  $\mathcal{N}(0, 1)$ , and  $x_i^{gen}$  drawn from RG(0, 1), and mean and mode refer to the type of point estimate used. We see that R-SBL performs significantly better than other methods. In fact, the average reconstruction error is less than 1% with R-SBL for cardinalities less than  $K = 45$ . Compared to the other algorithms, this is a significant improvement in reconstruction performance. Also note that, mean and mode point estimates have the same recovery performance.

We find that our method performs the best regardless of the distribution of  $\mathbf{x}^{gen}$  and outperforms other algorithms with a large margin. We summarize the MSE and PE for all other distributions of  $\mathbf{x}^{gen}$  in Table I for  $\Phi \sim \mathcal{N}(0, 1)$  and Table II for  $\Phi \sim \pm 1$  for a fixed cardinality of  $K = 50$ . We select  $K = 50$  because it is the most difficult experimental setting and because the relative performance of the tested algorithms is largely the same across different experimental settings as compared to Figures 2 and 3.

Table I and Table II show that the proposed method has superior recovery performance. The MSE for NN-Cauchy, NN-Laplace, Gamma and Chi-square are below 0.6% with the proposed method, whereas with SLEP and NN-OMP the

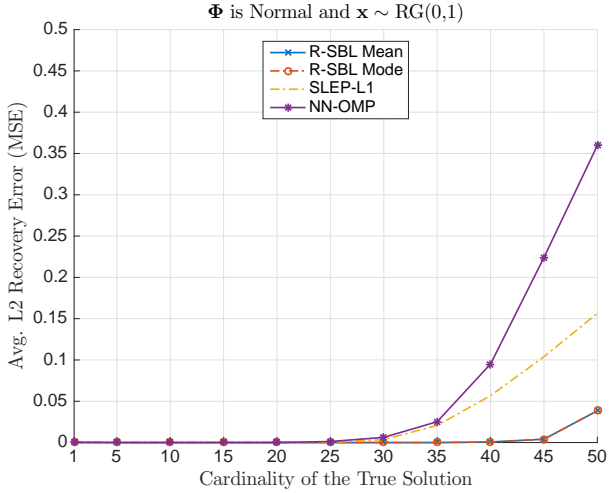


Fig. 2: Average MSE versus cardinality.  $\Phi$  is  $\mathcal{N}(\mathbf{0}, \mathbf{1})$  and  $\mathbf{x}^{gen}$  is  $\text{RG}(0, 1)$

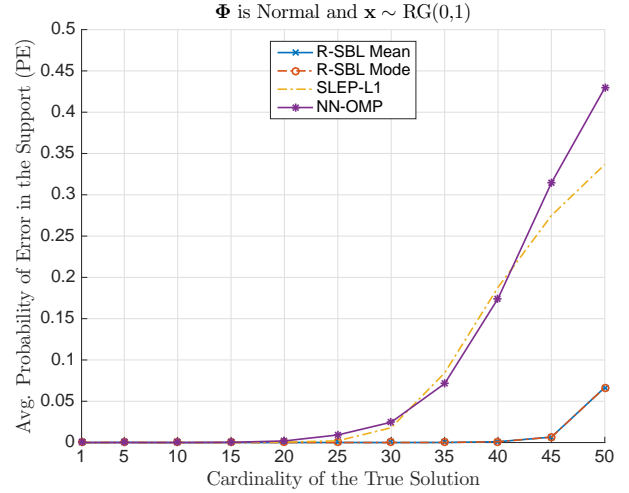


Fig. 3: Average PE versus cardinality.  $\Phi$  is  $\mathcal{N}(\mathbf{0}, \mathbf{1})$  and  $\mathbf{x}^{gen}$  is  $\text{RG}(0, 1)$

MSE is above 7%. Similar performance gains are observed in the PE. We also observe that the distribution of  $\Phi$  does not affect the results significantly and R-SBL is robust for different dictionary distributions. The worst performance is observed when  $\mathbf{x}^{gen}$  is Bernoulli with  $p(x_i^{gen} = 0.5) = 1/2$  and  $p(x_i^{gen} = 1.5) = 1/2$ . We see significantly larger MSE values with the greedy NN-OMP method, while SLEP- $\ell_1$  performs significantly better than NN-OMP. R-SBL performs much better compared to the other techniques, although the MSE and PE is relatively high compared to the results for the other distributions of  $\mathbf{x}^{gen}$ . This performance loss may result from the fact that the Bernoulli distribution is not approximated well by continuous sparsity-enforcing distributions.

*Noise Performance:* We now demonstrate the performance of the proposed method in the presence of Gaussian noise. The zero mean noise vector  $\mathbf{v}$  is added to measurements  $\mathbf{y}$  such that SNR is 20 dB. Selection of tuning parameters for NN-OMP, SLEP- $\ell_1$ , and R-SBL is not straightforward in the noisy simulations. To find a common ground between selecting these tuning parameters, we do line a search over the parameters for SLEP and NN-OMP and select the tuning-parameters that give the smallest MSE error over all cardinalities. For the R-SBL, we fix  $\sigma^2$  to be the true noise variance. It should be noted

that R-SBL is sensitive to the choice of  $\sigma^2$  and estimation of  $\sigma^2$  is a topic of research in its own. Depending on the application,  $\sigma^2$  can be estimated offline or estimation of  $\sigma^2$  can be incorporated into the R-SBL framework [31].

Figures 4 and 6 show the MSE and PE for Mean R-SBL and Mode R-SBL.  $\mathbf{x}_i^{gen}$  is drawn from  $\text{RG}(0, 1)$  and the elements of  $\Phi$  are drawn from  $\mathcal{N}(0, 1)$ . Compared to Figures 2 and 3, we see that noise degrades the recovery performance of each method. However, both Mean R-SBL and Mode R-SBL perform much better compared to SLEP- $\ell_1$  and NN-OMP, especially at larger cardinalities.

*Timing Performance:* The R-SBL algorithm we describe is computationally intensive compared to the greedy NN-OMP and convex SLEP- $\ell_1$  approaches. This is to be expected, as the EM inference computations in Algorithm 1 involve complex matrix operations such as Cholesky decomposition and inversion. Since certain applications require faster recovery at the expense of worse reconstruction, we discuss how R-SBL can be sped up. One way of achieving performance speed up is by pruning  $\gamma$  when its elements become close to zero. When an element  $\gamma_i$  becomes smaller than a threshold i.e.  $\epsilon_\gamma = 10^{-5}$ , we shrink  $\gamma$  and  $\Phi$  by ignoring the index  $i$  in the next iterations. This effectively reduces the problem

	Distribution of $\mathbf{x}^{gen}$	NN-OMP	SLEP	R-SBL
Avg. MSE	RG(0, 1)	0.3598	0.1564	<b>0.0384</b>
	NN-Cauchy(0, 1)	0.0069	0.0075	<b>0.0003</b>
	NN-Laplace(0, 1)	0.1109	0.0754	<b>0.0056</b>
	Gamma(1, 2)	0.1192	0.0760	<b>0.0036</b>
	Chi-square ( $\nu = 2$ )	0.1238	0.0778	<b>0.0037</b>
	Bernoulli	0.8671	0.2842	<b>0.2006</b>
Avg. PE	RG(0, 1)	0.4294	0.3367	<b>0.0667</b>
	NN-Cauchy(0, 1)	0.2221	0.3102	<b>0.0080</b>
	NN-Laplace(0, 1)	0.3054	0.3178	<b>0.0165</b>
	Gamma(1, 2)	0.3045	0.3209	<b>0.0122</b>
	Chi-square ( $\nu = 2$ )	0.3123	0.3252	<b>0.0135</b>
	Bernoulli	0.5508	0.3509	<b>0.2590</b>

TABLE I: Averaged MSE and PE Performance over 1000 trials for cardinality of  $K = 50$ .  $\Phi$  is distributed as  $\mathcal{N}(0, 1)$ .

	Distribution of $\mathbf{x}^{gen}$	NN-OMP	SLEP	R-SBL
Avg. MSE	RG(0, 1)	0.3660	0.1571	<b>0.0319</b>
	NN-Cauchy(0, 1)	0.0072	0.0075	<b>0.0002</b>
	NN-Laplace(0, 1)	0.1253	0.0759	<b>0.0054</b>
	Gamma(1, 2)	0.1227	0.0785	<b>0.0053</b>
	Chi-square ( $\nu = 2$ )	0.1280	0.0769	<b>0.0048</b>
	Bernoulli	0.8621	0.2918	<b>0.2229</b>
Avg. PE	RG(0, 1)	0.4331	0.3373	<b>0.0544</b>
	NN-Cauchy(0, 1)	0.2145	0.3073	<b>0.0062</b>
	NN-Laplace(0, 1)	0.3123	0.3219	<b>0.0176</b>
	Gamma(1, 2)	0.3132	0.3232	<b>0.0142</b>
	Chi-square ( $\nu = 2$ )	0.3130	0.3227	<b>0.0157</b>
	Bernoulli	0.5505	0.3547	<b>0.2788</b>

TABLE II: Averaged MSE and PE Performance over 1000 trials for cardinality of  $K = 50$ .  $\Phi$  is distributed as  $\pm 1$ .

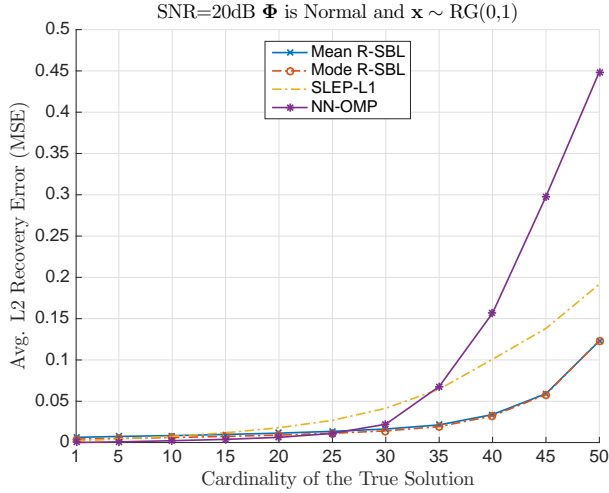


Fig. 4: Average MSE versus cardinality.  $\Phi$  is  $\mathcal{N}(\mathbf{0}, \mathbf{1})$  and  $\mathbf{x}^{gen}$  is  $\text{RG}(0, 1)$  and  $\mathbf{v}$  is Gaussian. SNR is 20 dB.

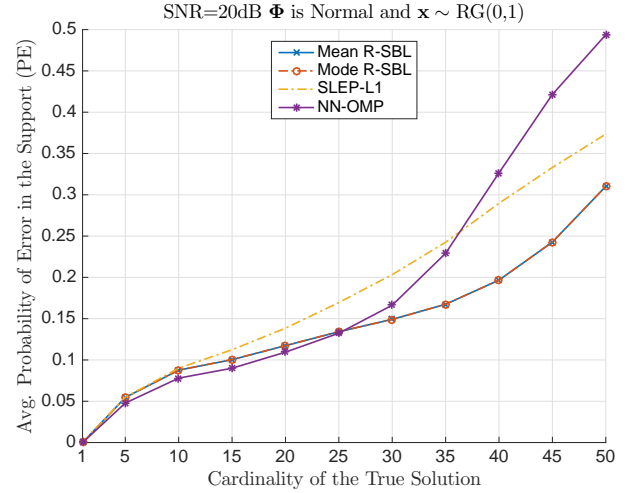


Fig. 6: Average PE versus cardinality.  $\Phi$  is  $\mathcal{N}(\mathbf{0}, \mathbf{1})$  and  $\mathbf{x}^{gen}$  is  $\text{RG}(0, 1)$  and  $\mathbf{v}$  is Gaussian. SNR is 20 dB.

dimensions and improves execution time. Alternatively, we can relax the convergence condition by making the  $\epsilon$  in Algorithm 1 larger, depending on the desired recovery MSE and PE.

Note that  $\text{SLEP}_{\ell_1}$  and NN-OMP will still run faster than R-SBL despite the speed-up considerations. Nevertheless, it should be noted that message passing techniques provide considerable speed-up in compressed sensing problems [45], [46], [47] and recent developments in message passing techniques for SBL [48] could be extended to the R-SBL framework, leading to significant speed-up.

Figure 5 shows an example of average execution times to solve the S-NNLS problem. This example includes both the pruning and the no-pruning methods. In the pruning method, we prune  $\gamma$  with a threshold of  $\epsilon_\gamma = 10^{-3}$  and the convergence condition is set to  $\epsilon = 10^{-5}$  in both cases. Results show pruning results in considerable speed-ups especially for  $K > 35$ . Depending on the desired recovery performance we can relax the pruning and convergence thresholds even more for further speed-up.

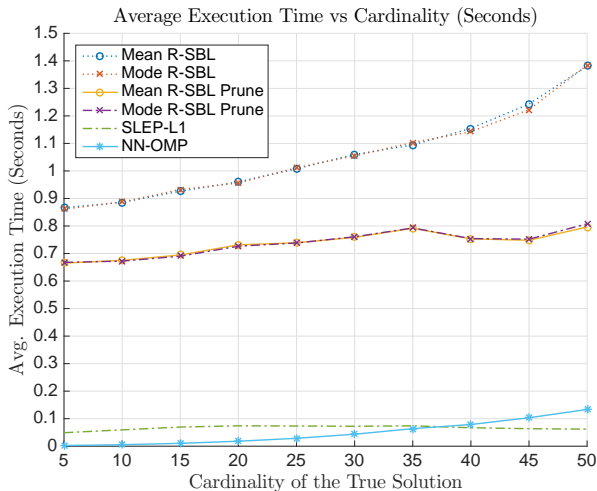


Fig. 5: Average Execution Time to Solve the S-NNLS Problem

## V. CONCLUSION

In this paper, we introduced a hierarchical Bayesian method to solve the S-NNLS problem. We developed the rectified Gaussian scale mixture model as a general and versatile prior to promote sparsity. We constructed the R-SBL algorithm using the EM framework and presented two point estimate methods for the EM framework, detailing the benefits and weaknesses of each. We fully derived the closed form expressions for the posterior of interest, which can be used in the future for a direct MAP estimation procedure instead of EM. We demonstrated that R-SBL outperforms the available S-NNLS solvers by a large margin both in terms of signal and support recovery. The performance gains achieved by R-SBL are consistent across different non-negative data distributions for  $\mathbf{x}$  and different sensing matrix distributions for  $\Phi$ . Under noisy conditions, we have shown that R-SBL is very robust in the MSE sense with both mean and mode point estimates and achieves a much better reconstruction performance compared to the other methods tested.

## VI. APPENDIX

We give the derivation of the posterior density  $p(\mathbf{x} | \mathbf{y}, \gamma)$  in Appendix VI-A. We detail the calculation of the first and second order moments of this density in Appendix VI-B. The closed-form posterior density  $p(\gamma | \mathbf{y})$  is derived in Appendix VI-C.

### A. Posterior Calculation

To calculate  $p(\mathbf{x} | \mathbf{y}, \gamma)$ , we use the chain rule and write

$$p(\mathbf{x} | \mathbf{y}, \gamma) = \frac{p(\mathbf{x}, \mathbf{y}, \gamma)}{p(\mathbf{y}, \gamma)} = \frac{p(\mathbf{y} | \mathbf{x}, \gamma)p(\mathbf{x} | \gamma)}{\int_{\mathbf{x}} p(\mathbf{y} | \mathbf{x}, \gamma)p(\mathbf{x} | \gamma)d\mathbf{x}}. \quad (28)$$

Note that, due to the Gaussian noise assumption,  $p(\mathbf{y} | \mathbf{x}, \gamma)$  is a Gaussian density. Since  $p(\mathbf{x} | \gamma)$  is a rectified Gaussian density, the numerator of (28) is a Gaussian multiplied by a

rectified Gaussian, which results in a rectified Gaussian density. Also, note that denominator is the normalizing constant so that we can write

$$p(\mathbf{x} | \mathbf{y}, \gamma) \propto c e^{-\frac{(\mathbf{x} - \boldsymbol{\mu})^T \boldsymbol{\Sigma}^{-1} (\mathbf{x} - \boldsymbol{\mu})}{2}} u(\mathbf{x}) \quad (29)$$

where  $c$  is the normalizing constant for the overall posterior density, obeying  $\int p(\mathbf{x} | \mathbf{y}, \gamma) d\mathbf{x} = 1$ , and  $\boldsymbol{\mu}$  and  $\boldsymbol{\Sigma}$  are given by (18) and (19), respectively. We want to calculate  $c$  to calculate the exact posterior. To do this, let  $\boldsymbol{\Sigma} = \mathbf{L}\mathbf{L}^T$  and  $\mathbf{r} = \mathbf{x} - \boldsymbol{\mu}$ , so that  $d\mathbf{x} = d\mathbf{r}$  and  $\boldsymbol{\Sigma}^{-1} = \mathbf{L}^{-T}\mathbf{L}^{-1}$ . Therefore, we can write

$$1 = \int_{-\infty}^{\infty} p(\mathbf{x} | \mathbf{y}, \gamma) d\mathbf{x} = c \int_{-\infty}^{\infty} e^{-\frac{-\mathbf{r}^T \mathbf{L}^{-T} \mathbf{L}^{-1} \mathbf{r}}{2}} d\mathbf{r}. \quad (30)$$

Now, let  $\mathbf{z} = \mathbf{L}^{-1}\mathbf{r}$ , which implies  $d\mathbf{r} = |\mathbf{L}|d\mathbf{z}$ , so that

$$1 = c|\mathbf{L}| \int_{-\beta}^{\infty} e^{-\frac{-\mathbf{z}^T \mathbf{z}}{2}} d\mathbf{z} = c|\mathbf{L}| \left(\frac{\pi}{2}\right)^{M/2} \prod_{i=1}^M \operatorname{erfc}\left(-\frac{\beta_i}{\sqrt{2}}\right) \quad (31)$$

where  $\beta = \mathbf{L}^{-1}\boldsymbol{\mu}$  is the lower limit of the new integral in vector form. Also, note that  $|\mathbf{L}| = |\boldsymbol{\Sigma}|^{1/2}$  since  $\mathbf{L}$  is a Cholesky factor of  $\boldsymbol{\Sigma}$ . Therefore, we obtain the normalizing constant of the ensemble posterior as

$$c = \frac{1}{|\boldsymbol{\Sigma}|^{1/2} \left(\frac{\pi}{2}\right)^{M/2} \prod_{i=1}^M \operatorname{erfc}\left(-\frac{\beta_i}{\sqrt{2}}\right)} \quad (32)$$

which enables us to write the posterior density as

$$p(\mathbf{x} | \mathbf{y}, \gamma) = \frac{e^{-\frac{(\mathbf{x} - \boldsymbol{\mu})^T \boldsymbol{\Sigma}^{-1} (\mathbf{x} - \boldsymbol{\mu})}{2}} u(\mathbf{x})}{|\boldsymbol{\Sigma}|^{1/2} \left(\frac{\pi}{2}\right)^{M/2} \prod_{i=1}^M \operatorname{erfc}\left(-\frac{\beta_i}{\sqrt{2}}\right)}. \quad (33)$$

### B. Moments

Given the exact posterior  $p(\mathbf{x} | \mathbf{y}, \gamma)$ , we want to calculate  $E_{\mathbf{x} | \mathbf{y}, \gamma, \sigma^2}[x_i^2]$ . We start by defining an auxiliary random variable,  $\tilde{\mathbf{x}}$ , which has distribution  $p(\tilde{\mathbf{x}}) = p(\mathbf{x} | \mathbf{y}, \gamma)$  and  $\mathbf{w}$ , which is related to  $\tilde{\mathbf{x}}$  by  $\tilde{\mathbf{x}} = \mathbf{L}\mathbf{w}$ , where  $\mathbf{L}$  is the Cholesky factor, defined as  $\boldsymbol{\Sigma} = \mathbf{L}\mathbf{L}^T$ , and is, by definition, invertible. Then, we can write the PDF of  $\mathbf{w}$  as

$$\begin{aligned} p(\mathbf{w}) &= |\mathbf{L}| p(\mathbf{x} | \mathbf{y}, \gamma) = c|\mathbf{L}| e^{-\frac{(\mathbf{w} - \boldsymbol{\beta})^T (\mathbf{w} - \boldsymbol{\beta})}{2}} u(\mathbf{w}) \\ &= \prod_{i=1}^M N^R(\beta_i, 1) = \prod_{i=1}^M p(w_i) \end{aligned} \quad (34)$$

Now, the covariance of  $\tilde{\mathbf{x}}$  can be expressed as

$$E[\tilde{\mathbf{x}}\tilde{\mathbf{x}}^T] = \mathbf{L}E[\mathbf{w}\mathbf{w}^T]\mathbf{L}^T. \quad (35)$$

Let  $\mathbf{R} = E[\mathbf{w}\mathbf{w}^T]$  be the covariance matrix of  $\mathbf{w}$ . The joint density of  $p(\mathbf{w})$  factors into the marginal densities  $p(w_i)$ , implying that each  $w_i$  is independent of  $w_j$  for  $i \neq j$ . As

a result, we can use the first and second moments of a single RG RV to fill  $\mathbf{R}$  as

$$R_{ij} = \begin{cases} E[w_i^2], & \text{if } i = j \\ E[w_i]E[w_j], & \text{otherwise} \end{cases} \quad (36)$$

where the first and second moments of the RG density are given by [38]

$$E[w_i] = \beta_i + \sqrt{\frac{2}{\pi}} \frac{e^{-\frac{\beta_i^2}{2}}}{\operatorname{erfc}\left(-\frac{\beta_i}{\sqrt{2}}\right)} \quad (37)$$

and

$$E[w_i^2] = \beta_i^2 + 1 + \sqrt{\frac{2}{2\pi}} \frac{\beta_i e^{-\frac{\beta_i^2}{2}}}{\operatorname{erfc}\left(-\frac{\beta_i}{\sqrt{2}}\right)}. \quad (38)$$

Finally, we can write

$$E_{\mathbf{x} | \mathbf{y}, \gamma, \sigma^2}[\mathbf{x}^2] = \operatorname{diag}(\mathbf{L}\mathbf{R}\mathbf{L}^T) \quad (39)$$

then  $E_{\mathbf{x} | \mathbf{y}, \gamma, \sigma^2}[x_i^2] = \operatorname{diag}(\mathbf{L}\mathbf{R}\mathbf{L}^T)_i$  and similarly the first moment is given by

$$E_{\mathbf{x} | \mathbf{y}, \gamma, \sigma^2}[\mathbf{x}] = \mathbf{L}E[\mathbf{w}]. \quad (40)$$

### C. Closed Form $p(\gamma | \mathbf{y})$

We start by observing that

$$p(\gamma | \mathbf{y}) = \frac{p(\mathbf{y} | \gamma)p(\gamma)}{p(\mathbf{y})}$$

Since  $p(\gamma)$  is generally chosen a-priori and  $p(\mathbf{y})$  is a normalizing constant which does not influence maximization of  $p(\gamma | \mathbf{y})$ , we turn to the computation of  $p(\mathbf{y} | \gamma)$ . Note that

$$p(\mathbf{y} | \gamma) = \int_{-\infty}^{\infty} p(\mathbf{y} | \mathbf{x}, \gamma)p(\mathbf{x} | \gamma)d\mathbf{x} \quad (41)$$

where  $p(\mathbf{x} | \gamma)$  is the RG distribution,  $p(\mathbf{y} | \mathbf{x}, \gamma)$  is a Gaussian distribution, and we use the shorthand  $d\mathbf{x}$  to represent integration over all of the elements of  $\mathbf{x}$ . Thus we can write

$$\begin{aligned} p(\mathbf{y} | \gamma) &= \int_{-\infty}^{\infty} e^{-\frac{|\mathbf{y} - \boldsymbol{\Phi}\mathbf{x}|^2}{2\sigma^2}} \frac{e^{-\frac{\mathbf{x}^T \boldsymbol{\Gamma}^{-1} \mathbf{x}}{2}}}{(2\pi\sigma^2)^{N/2} (2\pi)^{M/2} |\boldsymbol{\Gamma}|^{1/2}} u(\mathbf{x}) d\mathbf{x} \\ &= \frac{\sigma^{-N}}{(2\pi)^{(N+M)/2} |\boldsymbol{\Gamma}|^{1/2}} \int_0^{\infty} e^{-\frac{\psi}{2}} d\mathbf{x} \end{aligned} \quad (42)$$

where  $\boldsymbol{\Gamma} = \operatorname{diag}(\gamma)$  and  $\psi$  is the exponent we would like to focus on. Before proceeding let  $\tilde{\boldsymbol{\Sigma}} = (\boldsymbol{\Phi}^T \boldsymbol{\Phi} / \sigma^2 + \boldsymbol{\Gamma}^{-1})^{-1}$  and  $\boldsymbol{\mu} = \tilde{\boldsymbol{\Sigma}} \boldsymbol{\Phi}^T \mathbf{y} / \sigma^2$ . Then, it can be shown that

$$\psi = \frac{\mathbf{y}^T (\sigma^2 \mathbf{I} - \boldsymbol{\Phi} \tilde{\boldsymbol{\Sigma}} \boldsymbol{\Phi}^T) \mathbf{y}}{\sigma^4} + (\mathbf{x} - \boldsymbol{\mu})^T \tilde{\boldsymbol{\Sigma}}^{-1} (\mathbf{x} - \boldsymbol{\mu}) \quad (43)$$

To simplify the expression, we re-write  $\tilde{\boldsymbol{\Sigma}}$  as:

$$\tilde{\boldsymbol{\Sigma}} = \left(\frac{\boldsymbol{\Phi}^T \boldsymbol{\Phi}}{\sigma^2} + \boldsymbol{\Gamma}^{-1}\right)^{-1} = \boldsymbol{\Gamma} - \boldsymbol{\Gamma} \boldsymbol{\Phi}^T (\boldsymbol{\Phi} \boldsymbol{\Gamma} \boldsymbol{\Phi}^T + \sigma^2 \mathbf{I})^{-1} \boldsymbol{\Phi} \boldsymbol{\Gamma} \quad (44)$$

Using (44), we can simplify the  $\sigma^2 \mathbf{I} - \Phi \tilde{\Sigma} \Phi^T$  term in (43) to:

$$-\Phi \tilde{\Sigma} \Phi^T + \sigma^2 \mathbf{I} = \sigma^4 (\Phi \Gamma \Phi^T + \sigma^2 \mathbf{I})^{-1}. \quad (45)$$

Now, using (45), we can write  $\psi$  as

$$\psi = \mathbf{y}^T \Sigma_{\mathbf{y}}^{-1} \mathbf{y} + (\mathbf{x} - \boldsymbol{\mu})^T \tilde{\Sigma}^{-1} (\mathbf{x} - \boldsymbol{\mu}) \quad (46)$$

where  $\Sigma_{\mathbf{y}} = \Phi \Gamma \Phi^T + \sigma^2 \mathbf{I}$ . Then using (46), we rewrite (42) as

$$p(\mathbf{y} | \gamma) = \frac{\sigma^{-N} e^{-\mathbf{y}^T \Sigma_{\mathbf{y}}^{-1} \mathbf{y} / 2}}{(2\pi)^{(N+M)/2} |\Gamma|^{1/2}} \int_0^\infty e^{-(\mathbf{x} - \boldsymbol{\mu})^T \tilde{\Sigma}^{-1} (\mathbf{x} - \boldsymbol{\mu}) / 2} dx \quad (47)$$

Note that the integral in Equation (47) is the integral of the exponent part of the rectified Gaussian density. This is already computed in (30) through (32) as the inverse normalizing constant  $1/c$  of the RG density. Thus, using (32) in (47), we can write

$$p(\mathbf{y} | \gamma) = \frac{\sigma^{-N} e^{-\frac{\mathbf{y}^T \Sigma_{\mathbf{y}}^{-1} \mathbf{y}}{2}} \prod_{i=1}^M \operatorname{erfc}\left(-\frac{\tilde{\beta}_i}{\sqrt{2}}\right)}{2^M (2\pi)^{N/2} |\Gamma \tilde{\Sigma}^{-1}|^{1/2}} \quad (48)$$

where  $\tilde{\beta}_i$  is the  $i$ 'th element of  $\tilde{\boldsymbol{\beta}} = \tilde{\mathbf{L}} \boldsymbol{\mu}$ , with  $\tilde{\mathbf{L}}$  defined as the Cholesky factor  $\tilde{\Sigma} = \tilde{\mathbf{L}} \tilde{\mathbf{L}}^T$ . With some manipulation, we can further simplify (48) using

$$|\Gamma \tilde{\Sigma}^{-1}|^{1/2} = \sigma^{-n} |\Sigma_{\mathbf{y}}|^{1/2}. \quad (49)$$

Combining (48) and (49), we have

$$p(\mathbf{y} | \gamma) = \frac{e^{-\frac{\mathbf{y}^T \Sigma_{\mathbf{y}}^{-1} \mathbf{y}}{2}} \prod_{i=1}^M \operatorname{erfc}\left(-\frac{\tilde{\beta}_i}{\sqrt{2}}\right)}{\sqrt{(2\pi)^N |\Sigma_{\mathbf{y}}|} 2^M}. \quad (50)$$

## REFERENCES

- [1] C. L. Lawson and R. J. Hanson, *Solving least squares problems*. SIAM, 1974, vol. 161.
- [2] B. M. Jedynek and S. Khudanpur, "Maximum likelihood set for estimating a probability mass function," *Neural computation*, vol. 17, no. 7, pp. 1508–1530, 2005.
- [3] J. P. Vila and P. Schniter, "An empirical-bayes approach to recovering linearly constrained non-negative sparse signals," *Signal Processing, IEEE Transactions on*, vol. 62, no. 18, pp. 4689–4703, 2014.
- [4] R. Peharz and F. Pernkopf, "Sparse nonnegative matrix factorization with 0-constraints," *Neurocomputing*, vol. 80, pp. 38–46, 2012.
- [5] H. Kim and H. Park, "Sparse non-negative matrix factorizations via alternating non-negativity-constrained least squares for microarray data analysis," *Bioinformatics*, vol. 23, no. 12, pp. 1495–1502, 2007.
- [6] H. Kim and H. Park, "Nonnegative matrix factorization based on alternating nonnegativity constrained least squares and active set method," *SIAM Journal on Matrix Analysis and Applications*, vol. 30, no. 2, pp. 713–730, 2008.
- [7] V. P. Pauca, F. Shahnaz, M. W. Berry, and R. J. Plemmons, "Text mining using non-negative matrix factorizations." in *SDM*, vol. 4, 2004, pp. 452–456.
- [8] V. Monga and M. K. Mihčak, "Robust and secure image hashing via non-negative matrix factorizations," *Information Forensics and Security, IEEE Transactions on*, vol. 2, no. 3, pp. 376–390, 2007.
- [9] P. C. Loizou, "Speech enhancement based on perceptually motivated bayesian estimators of the magnitude spectrum," *Speech and Audio Processing, IEEE Transactions on*, vol. 13, no. 5, pp. 857–869, 2005.
- [10] C. Févotte, N. Bertin, and J.-L. Durrieu, "Nonnegative matrix factorization with the itakura-saito divergence: With application to music analysis," *Neural computation*, vol. 21, no. 3, pp. 793–830, 2009.
- [11] P. Sajda, S. Du, T. R. Brown, R. Stoyanova, D. C. Shungu, X. Mao, and L. C. Parra, "Nonnegative matrix factorization for rapid recovery of constituent spectra in magnetic resonance chemical shift imaging of the brain," *Medical Imaging, IEEE Transactions on*, vol. 23, no. 12, pp. 1453–1465, 2004.
- [12] L. C. Potter, E. Ertin, J. T. Parker, and M. Cetin, "Sparsity and compressed sensing in radar imaging," *Proceedings of the IEEE*, vol. 98, no. 6, pp. 1006–1020, 2010.
- [13] A. Hurmalainen, R. Saeidi, and T. Virtanen, "Group sparsity for speaker identity discrimination in factorisation-based speech recognition." in *INTERSPEECH*, 2012.
- [14] M. Lustig, J. M. Santos, D. L. Donoho, and J. M. Pauly, "kt sparse: High frame rate dynamic mri exploiting spatio-temporal sparsity," in *Proceedings of the 13th Annual Meeting of ISMRM, Seattle*, vol. 2420, 2006.
- [15] M. Elad, *Sparse and Redundant Representations*. Springer New York, 2010.
- [16] Y. C. Eldar and G. Kutyniok, *Compressed sensing: theory and applications*. Cambridge University Press, 2012.
- [17] Y. C. Pati, R. Rezaifar, and P. Krishnaprasad, "Orthogonal matching pursuit: Recursive function approximation with applications to wavelet decomposition," in *Signals, Systems and Computers, 1993. 1993 Conference Record of The Twenty-Seventh Asilomar Conference on*. IEEE, 1993, pp. 40–44.
- [18] A. M. Bruckstein, D. L. Donoho, and M. Elad, "From sparse solutions of systems of equations to sparse modeling of signals and images," *SIAM review*, vol. 51, no. 1, pp. 34–81, 2009.
- [19] J. Nocedal and S. Wright, *Numerical optimization*. Springer Science & Business Media, 2006.
- [20] S. Boyd and L. Vandenberghe, *Convex optimization*. Cambridge university press, 2004.
- [21] C.-b. Lin, "Projected gradient methods for nonnegative matrix factorization," *Neural computation*, vol. 19, no. 10, pp. 2756–2779, 2007.
- [22] P. O. Hoyer, "Non-negative matrix factorization with sparseness constraints," *The Journal of Machine Learning Research*, vol. 5, pp. 1457–1469, 2004.
- [23] P. D. Grady and S. T. Rickard, "Compressive sampling of non-negative signals," in *Machine Learning for Signal Processing, 2008. MLSP 2008. IEEE Workshop on*. IEEE, 2008, pp. 133–138.
- [24] R. Chartrand and W. Yin, "Iteratively reweighted algorithms for compressive sensing," in *Acoustics, speech and signal processing, 2008. ICASSP 2008. IEEE international conference on*. IEEE, 2008, pp. 3869–3872.
- [25] R. Giri and B. D. Rao, "Type I and Type II Bayesian Methods for Sparse Signal Recovery using Scale Mixtures," *arXiv preprint arXiv:1507.05087*, 2015.
- [26] D. F. Andrews and C. L. Mallows, "Scale mixtures of normal distributions," *Journal of the Royal Statistical Society. Series B (Methodological)*, pp. 99–102, 1974.
- [27] A. P. Dempster, N. M. Laird, and D. B. Rubin, "Maximum likelihood from incomplete data via the em algorithm," *Journal of the royal statistical society. Series B (methodological)*, pp. 1–38, 1977.
- [28] A. P. Dempster, N. M. Laird, and D. B. Rubin, "Iteratively reweighted least squares for linear regression when errors are normal/independent distributed," 1980.
- [29] K. Lange and J. S. Sinsheimer, "Normal/independent distributions and their applications in robust regression," *Journal of Computational and Graphical Statistics*, vol. 2, no. 2, pp. 175–198, 1993.
- [30] M. E. Tipping, "Sparse bayesian learning and the relevance vector machine," *The journal of machine learning research*, vol. 1, pp. 211–244, 2001.
- [31] D. P. Wipf and B. D. Rao, "An empirical bayesian strategy for solving the simultaneous sparse approximation problem," *Signal Processing, IEEE Transactions on*, vol. 55, no. 7, pp. 3704–3716, 2007.
- [32] J. A. Palmer, "Variational and scale mixture representations of non-gaussian densities for estimation in the bayesian linear model: Sparse coding, independent component analysis, and minimum entropy segmentation," 2006.
- [33] J. Palmer, K. Kreutz-Delgado, B. D. Rao, and D. P. Wipf, "Variational em algorithms for non-gaussian latent variable models," in *Advances in neural information processing systems*, 2005, pp. 1059–1066.
- [34] E. L. Lehmann and G. Casella, *Theory of point estimation*. Springer Science & Business Media, 1998, vol. 31.

- [35] D. P. Wipf, B. D. Rao, and S. Nagarajan, "Latent variable bayesian models for promoting sparsity," *Information Theory, IEEE Transactions on*, vol. 57, no. 9, pp. 6236–6255, 2011.
- [36] R. Schachtner, G. Poeppel, A. Tomé, and E. Lang, "A bayesian approach to the lee-seung update rules for nmf," *Pattern Recognition Letters*, vol. 45, pp. 251–256, 2014.
- [37] M. Harva and A. Kabán, "Variational learning for rectified factor analysis," *Signal Processing*, vol. 87, no. 3, pp. 509–527, 2007.
- [38] J. W. Miskin, "Ensemble learning for independent component analysis," in *Advances in Independent Component Analysis*. Citeseer, 2000.
- [39] M. A. Figueiredo, "Adaptive sparseness for supervised learning," *Pattern Analysis and Machine Intelligence, IEEE Transactions on*, vol. 25, no. 9, pp. 1150–1159, 2003.
- [40] D. P. Wipf and B. D. Rao, "Sparse bayesian learning for basis selection," *Signal Processing, IEEE Transactions on*, vol. 52, no. 8, pp. 2153–2164, 2004.
- [41] Z. Zhang, T.-P. Jung, S. Makeig, Z. Pi, and B. Rao, "Spatiotemporal sparse bayesian learning with applications to compressed sensing of multichannel physiological signals," *Neural Systems and Rehabilitation Engineering, IEEE Transactions on*, vol. 22, no. 6, pp. 1186–1197, 2014.
- [42] B. Hajek, *Random Processes for Engineers*. Cambridge University Press, 2015.
- [43] J. Liu, S. Ji, J. Ye *et al.*, "Slep: Sparse learning with efficient projections," *Arizona State University*, vol. 6, p. 491, 2009.
- [44] A. M. Bruckstein, M. Elad, and M. Zibulevsky, "On the uniqueness of nonnegative sparse solutions to underdetermined systems of equations," *Information Theory, IEEE Transactions on*, vol. 54, no. 11, pp. 4813–4820, 2008.
- [45] J. P. Vila and P. Schniter, "Expectation-maximization gaussian-mixture approximate message passing," *Signal Processing, IEEE Transactions on*, vol. 61, no. 19, pp. 4658–4672, 2013.
- [46] D. L. Donoho, A. Maleki, and A. Montanari, "Message-passing algorithms for compressed sensing," *Proceedings of the National Academy of Sciences*, vol. 106, no. 45, pp. 18 914–18 919, 2009.
- [47] D. L. Donoho, A. Maleki, and A. Montanari, "Message passing algorithms for compressed sensing: I. motivation and construction," in *Information Theory Workshop (ITW), 2010 IEEE*. IEEE, 2010, pp. 1–5.
- [48] M. Al-Shoukairi and B. Rao, "Sparse bayesian learning using approximate message passing."